Supplementary Material (ESI) for Lab on a Chip

An Integrated Optics Microfluidic Device For Detecting Single DNA Molecules

Jeffrey R. Krogmeier,[a]* Ian Schaefer,[a] George Seward,[b] Gregory R. Yantz,[a] and Jonathan W. Larson[a]

[a]U.S. Genomics Inc., 12 Gill Street, Suite 4700, Woburn, MA 01801 USA
[b]L-A-Omega Inc., 20 Central Street, Arlington, MA 02476 USA

* *jkrogmeier@usgenomics.com*

Collector - Optical Design

The fluorescence collection efficiency of the collector mirror is primarily determined by the microfluidic channel dimensions. As displayed in Fig. S1a, the diagonal from the center of the fluid-filled (buffer/H_2O, $n_d = 1.333$) microfluidic channel (5 μm x 1 μm) to the corner defines the maximum collection half-angle as 77.8º limiting the *marginal* numerical aperture (NA) of the device to 1.30 (NA = 1.333 sin 77.8°).[†] The fluorescence emitted over this angle enters the fused silica (fused silica, $n_d = 1.458$) above the channel at a maximum angle of 63.7° from normal due to refraction at the water/fused silica interface as shown in Fig. S1a. The collector mirror, also made of fused silica, does not alter the light collection pathway and the NA remains 1.30 (NA = 1.458 sin 63.7°).[‡] In addition, the collector perimeter height, *h* in Fig. S1b, was optimized for maximum collection efficiency over the expected maximum entrance angle (63.7°).

The vision lens (4 mm diameter, 8 mm effective focal length) at the crest of the collector mirror, enables the alignment of the laser spot within the microfluidic channel to be monitored (see Component Integration in manuscript text) and also provides an optical path for the extraneous excitation light to exit the integrated optics device away from the detector. The vision lens diameter is oversized with regard to the expected divergence diameter of the excitation source at the vision lens crest (4 mm *vs.* 0.94 mm full width

[†] The angle from the microfluidic channel center to the corner is 78.7°; however, 77.8° was chosen to minimize scattering effects at the microfluidic channel corner during the modeling process.

[‡] The numerical aperture (NA) of a lens is defined as, NA = n sin θ, where n is the refractive index of the medium and θ is the half-angle of the aperture with respect to the object or image. The NA is invariant between two refractive media due to Snell's Law. Therefore, a collection angle within any portion of the collector may be derived from the invariant NA and the local refractive index.

half maximum, FWHM, respectively) to minimize back reflection toward the detector. However, the vision lens position in the center of the collector mirror decreases the collection efficiency by allowing fluorescence emitted towards this position to escape through the vision lens. The magnitude of the fluorescence collection loss is defined by the angle between the optical axis of the collector and the vision lens perimeter (19°), as depicted in Fig. S1b, and results in a central loss of 0.48 NA (NA = 1.458 sin 19°). The difference between the marginal NA (1.30) and central NA (0.48) represents an *annular* NA of the collector of 0.82. However, the collection efficiency of an annular NA of 0.82 is highly dependent upon the magnitude of the marginal NA, that is, the collection efficiency of an annular NA of 0.82 with a marginal NA of 1.30 displays significantly higher collection efficiency than that of a marginal NA of 0.82 only. Therefore, the annular NA of 0.82 is misleading as a numerical representation of the collector mirror performance. Rather, the performance of the collector mirror can be more accurately expressed in terms of the hemispherical collection efficiency (HCE):

$$HCE = 1 - \cos \theta$$

where θ corresponds to the angle from the optical axis of the collector mirror to its margin. The HCE is derived from the expression for calculating the solid angle of a cone. Due to the nonlinear increase in HCE, it becomes obvious that a collector mirror with an *annular* NA of 0.82 would display significantly greater collection efficiency than a collector mirror with a central NA of 0.82. For example, the marginal collection efficiency of the collector mirror within water represents 78% of a hemisphere (1 - cos 77.8°). The vision lens in the center of the collector mirror crest subtends a circa 19º half-angle in fused silica (NA = 1.458 sin 19°) and 21º at the fluid-filled channel (NA =

1.333 sin 21°) comprising a NA loss of 0.48. However, this loss of NA accounts for only a 7% loss (1 - cos 21°) in terms of HCE of the collector mirror. Therefore, the total collection efficiency of the collector mirror represents 71% of a hemisphere. In comparison, a marginal NA of 0.82 only represents a 21% (1 - cos 38°) HCE.

Currently, the HCE of the collector mirror is limited to 71% by the dimensions of the microfluidic channel (5 μm x 1 μm) and the position of the vision lens in the center of the collector mirror. In the current channel geometry, the 77.8º angle from the channel center to the corner defines the angle over which the fluorescence photons are collected from the channel. Theoretically, widening the microfluidic channel while maintaining the same depth leads to a significant increase in the HCE. However, as the channel gets wider, the fluorescence photons begin to reflect due to the flat incident angle rather than transmit through the fused silica toward the collector mirror leading to a loss in collection. This situation also exists for the extended length of the microfluidic channel (*i.e.* the fluid flow axis) in the interrogation region. However, the extended channel represents only a small fraction of the collection angle and was therefore ignored during the modeling process. Conversely, employing a deeper channel while keeping the same width, leads to a significant loss in HCE and is not advantageous to fluorescence collection.

As previously described, fluorescence photons that move from the lower refractive index water/buffer (n_d = 1.333) in the microfluidic channel to the higher refractive index fused silica cover plate (n_d = 1.458) within 77.8°are bent towards the normal at 63.7°. This reduction in the collection angle is beneficial to the collection efficiency by decreasing the effect of axial de-focus and lateral de-center of the collector mirror position. Photons that exit the microfluidic channel between 77.8º and 102.2º, the

angle between the channel center and the upper and lower corners of the microfluidic channel, respectively, in Fig. S1a, exit the side of the microfluidic channel at an angle of 12.2º or less. These photons are likely contained by total internal reflection until exiting through the side of the microfluidic device. Photons between 102.2º and 180º exit the microfluidic channel floor toward the illuminator lens. These photons are also likely contained by total internal reflection until exiting through the edge of illuminator flat or through the illuminator lens. These extraneous photons could theoretically return to the collection zone as unwanted background, however, the effect is presumed insignificant.

An added benefit of using a reflective optic for fluorescence collection, as opposed to a refractive optic, is the absence of chromatic aberrations in the reflected fluorescence. Furthermore, the monolithic refractive index of the collector mirror defines a parabola as the perfect aspheric profile for reflection whereas a spherical reflector profile would create gross aberrations. Theoretically, the reflected fluorescence exits the collector without aberration in a collimated manner towards the detector. However, finite fabrication tolerances limit the collimation quality by introducing aberrations, such as spherical aberration, coma, astigmatism, and lateral color, all of which were carefully considered during the design process.[§] For example, the performance of the collector mirror is highly dependent upon thickness and positional tolerances. Deviations from nominal thickness in either the collector mirror or the fused silica cover plate over the microfluidic channel create significant spherical aberration. Deviation in the alignment of the collector mirror relative to the microfluidic channel creates significant coma, and a slight astigmatism and lateral color aberration in the reflected fluorescence. The lateral color aberration is created by fluorescence passing through the illuminator flat at an off-

[§] E. Hecht, *Optics*, Addison Wesley, San Francisco, 4th edition, 2002.

normal incidence angle created by the misalignment of the collector mirror and microfluidic channel. Due to the large NA (NA = 1.30) at the collector mirror margin, small deviations in thickness and centering of the optical components lead to degradation of the collimation quality of the collected fluorescence.

The thickness tolerance or distance from the microfluidic channel to the crest of the parabolic profile of the collector mirror is held within +125/-75 μm by known manufacturing tolerances. This tolerance range is defined by +100/-50 μm tolerances from the plano face of the collector mirror to its crest (5.35 mm) and a ±25 μm tolerance on the 500 μm fused silica wafer. Spherical aberrations occur in the reflected fluorescence when the thickness tolerance deviates from nominal. For example, a +125 μm thickness error creates a *convergence* of 31 milliradians in the reflected collimated fluorescence while conversely an error of -75 μm creates 23 milliradians of *divergence*. The magnitude of collector de-center is difficult to quantify so assumptions were made in order to estimate its affect. The collector mirror is currently positioned relative to the microfluidic channel using an alignment jig. The vision lens is then employed as an objective lens in combination with a microscope tube lens and CCD camera (see Component Integration in manuscript text) to monitor the alignment of the collector mirror relative to the microfluidic channel. However, the vision lens and collector mirror are fabricated independently due to manufacturing limitations and then bonded together within 50 μm of center. Ideally, the vision lens and collector would comprise a monolithic block of fused silica to eliminate this tolerance. In addition, an *assumed* angular tolerance in the microscope body of 0.1º produces an additional 14 μm of collector mirror de-center relative to the microfluidic channel. Thus, the total collector

de-center relative to the microfluidic channel is estimated to be 64 μm through the sum of the vision lens and collector mirror de-center, and the *assumed* angular tolerance in the microscope during collector positioning. A 64 μm de-center creates coma resulting in an error of 10 milliradians in deflection of the collimated fluorescence. The cumulative effect of the thickness and de-center tolerances create aberrations that degrade the collimation quality of the reflected fluorescence. Aberrations in the reflected fluorescence caused by imperfect tolerances can be compensated for by using a large area detector (see Testing Apparatus in manuscript text). However, a large area detector also enables unwanted background to more readily reach the detector and can degrade the performance of the integrated device.

Illuminator - Performance

The illuminator lens has a relatively low NA of 0.10; however, since the illuminator is not used for light collection, the primary impact of the low NA is on the spatial resolution of the measurement. The predicted point spread function (PSF) of the illuminator lens is 2.0 μm (FWHM) at the microfluidic channel. Experimentally, the PSF of the illuminator was determined by delivering collimated 532 nm laser light (0.48 mm diameter FWHM) to the illuminator lens (4.0 mm diameter) using the fiber optic positioned in the coupler and focusing the laser light by iterative positioning of the illuminator assembly relative to the microfluidic channel. The laser spot was then imaged onto a CCD camera using the vision lens system (see Component Integration in text). The results are presented in Fig. S2a. In order to determine the laser spot size, the image pixel dimensions were calibrated by bright field imaging using known distances

between microfluidic features and determined to be 0.619 μm / pixel. This enabled the experimental PSF of the focused laser spot in Fig. S2a to be determined. Horizontal and vertical cross-sections of the imaged laser spot, presented in Figs. S2b and S2c respectively, reveal a highly symmetric line profile with a horizontal cross section of 2.02 μm and vertical cross section of 2.00 μm at FWHM. In addition, fitting the cross-sections with a Gaussian function reveals R^2 values greater than 0.99 for both dimensions confirming the Gaussian nature of the laser spot. An optical resolution limit of 2.0 μm is sufficient for probing stretched λ-phage DNA molecules with expected contour lengths of 16 μm (48.5 kb, 3.4 Å / DNA base).[**]

[**] R. R. Sinden, *DNA Structure and Function*, Academic Press, San Diego, 1994.

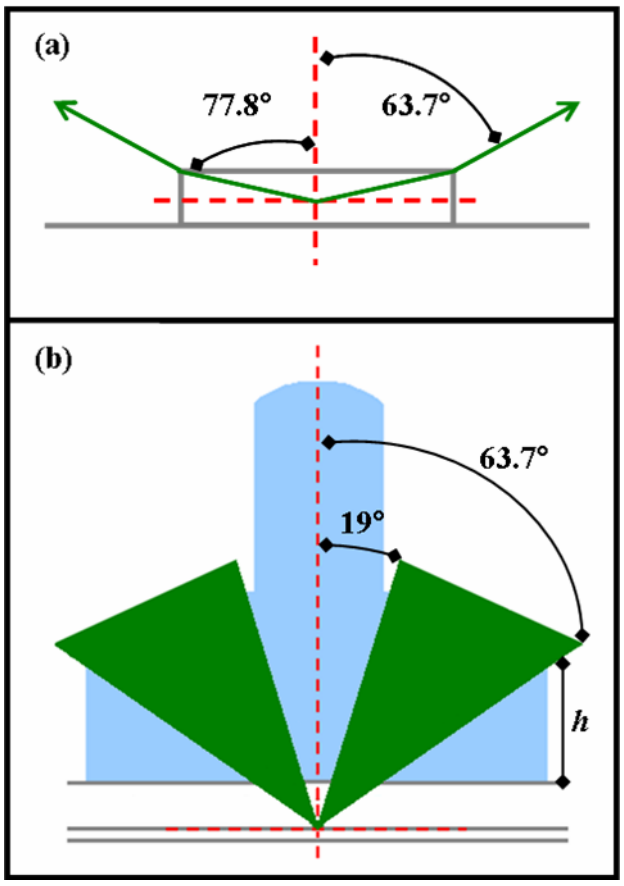

Fig. S1 Schematic of the fluorescence collection pathway in the integrated optics microfluidic device. (a) Fluorescence collection angles within the microfluidic channel presented as a cross-section with sample flow going into the page. Gray lines: fused silica boundaries around the rectangular channel (5 µm x 1 µm) and between the etched substrate and bonded fused silica cover; Red dashed lines: bisection of the microfluidic channel; Green rays: marginal fluorescence rays originating from the center of the microfluidic channel that refract toward the normal at the water/fused silica interface. (b) Fluorescence propagation (green) through the microfluidic device (outlined in gray) and collector mirror (solid blue). Red dashed lines: same as (a).

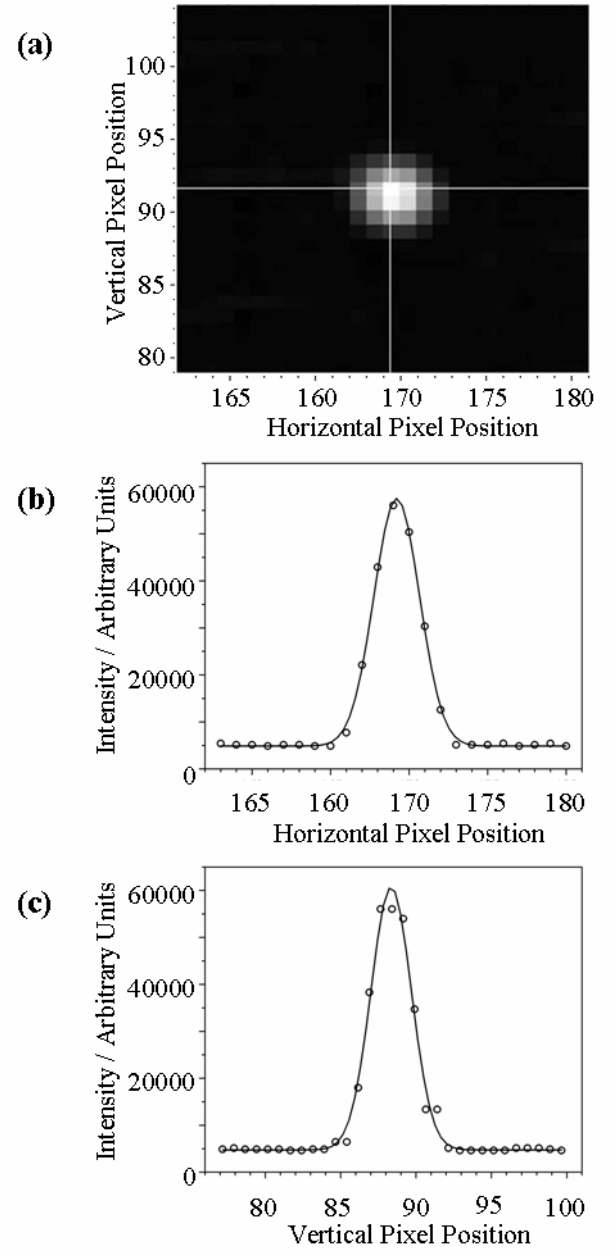

Fig. S2 (a) An image of the focused laser spot in the microfluidic channel. A horizontal (b) and vertical (c) cross section of the focused laser spot in (a). The circles represent the data points extracted from (a) and the solid line is a best fit Gaussian function to the data. The horizontal and vertical cross-sections fit a Gaussian profile of 2.02 μm and 2.00 μm at FWHM, respectively, with an R^2 fit greater than 0.99 in both dimensions demonstrating the symmetric Gaussian nature of the focused laser spot.